

Impact Containment Barriers with Geotextile Tubes

Flávio da Silva Ornelas^{1*}, Luís Fernando Martins Ribeiro², Rafael Cerqueira Silva²

¹Instituto Federal de Educação Ciência e Tecnologia—IFTO, Palmas, Brasil

²Departamento de Engenharia Civil e Ambiental, Programa de pós graduação em Geotecnia, Universidade de Brasília—UnB/Campus Universitário Darcy Ribeiro, Brasília, Brasil

Email: *flavioornelas@ifto.edu.br, lmartins@unb.br, rafael.silva@unb.br

How to cite this paper: Ornelas, F. S., Ribeiro, L. F. M., & Silva, R. C. (2024). Impact Containment Barriers with Geotextile Tubes. *Journal of Geoscience and Environment Protection*, 12, 325-344. <https://doi.org/10.4236/gep.2024.125018>

Received: April 4, 2024

Accepted: May 28, 2024

Published: May 31, 2024

Copyright © 2024 by author(s) and Scientific Research Publishing Inc. This work is licensed under the Creative Commons Attribution International License (CC BY 4.0).

<http://creativecommons.org/licenses/by/4.0/>



Open Access

Abstract

Recently, tragic tailings dam collapses in Brazil have caused deaths and major destruction and the need to develop technologies capable of preventing damage to people and the environment. Brazilian tailings dams are in a situation of uncertainty due to new legislation that even requires decommissioning, an activity that involves many problems and where the risk of failure is the main one. An impact containment structure downstream of these dams can be effective and geotextile tubes, in a new approach, have emerged as an option with advantages in terms of execution, costs and safety. The technology is versatile and can bring many benefits such as the reuse of tailings or filling with low-energy or reused materials. In this research, geotextile tubes were tested as free containment barriers, experiencing impacts in reduced models. The safety factor for the stability of the structure was constructed using an equation which is the ratio between the self-weight of the barrier structure and its coefficient of static friction and the impact pressure, where the data showed an adequate correlation which suggests the viability of mitigating risks.

Keywords

Geotextile Tube, Debris Flow, Barriers, Impact, Mining

1. Introduction

Safety technologies are always being developed and updated so that different events don't claim lives or cause major environmental and financial damage. Recently, tragic tailings dam collapses in Brazil and around the world have caused deaths and great destruction. New structures such as impact containment dams

may be able to minimize the consequences and mitigate the problems of a possible failure. Geotextile tubes have emerged as a new option with enormous potential benefits in terms of execution, costs and safety, with a technology that is gaining its due to solve various complex problems.

With a new approach, geotextile tubes can be used as barriers to slow down or stop materials and impacts caused by a breach of a dam of various accumulations or by a mass movement such as a debris flow. This new possible use can be determined as an Impact Containment Barrier. The research experimented with the technology by simulating the impacts and behavior characteristics of the structure of geotextile tubes used as impact containment barriers.

Geotextile tubes are made up of pockets of geotextile filled with dredgeable materials that consolidate and thus form gravity structures, which can be used for a variety of purposes. Their strengths and first studies were developed by [Leshchinsky et al. \(1996\)](#), [Pilarczyk \(2000\)](#), and the main uses, characteristics, materials, dimensions and uses were explored by authors such as [Pilarczyk \(2000\)](#), [Lawson \(2008\)](#). [Pilarczyk \(2000\)](#), studied the uses and forms of execution, construction of structures in specific locations where they are exposed to more severe waves and current attacks (artificial islands, breakwaters, river and sea dykes, waterways and inlet channels with greater intensity and loading due to navigation, etc.) and also the stress concentrations during filling and points of attention. [Lawson \(2008\)](#) defined the engineering parameters for dimensioning these structures and their main functions. [Pilarczyk \(2000\)](#) and [Lawson \(2008\)](#) also evaluated the effect of foundation settlement, where geotextile tubes are constructed in compressible foundations and are required to meet specific height requirements for hydraulic structures (e.g. breakwaters).

The versatility of this technology is mainly due to the fact that it can be better adapted and implemented in places where it is difficult to use other structures, avoiding earthquakes induced by construction processes and even the low bearing capacity of the foundation. It is widely used for containment and for restoring areas, such as the work described by [Yee et al. \(2007\)](#) of the artificial island that was built to provide a construction platform over shallow areas for the great Incheon Bridge connecting the city of Songdo in the Incheon Free Economic Zone and Incheon International Airport, located on Yongjong Island in South Korea, with the technique of containment dyke cores where the water depth is relatively shallow and the other side is filled hydraulically or dry, forming islands or recovering flooded areas.

Several authors have described debris flows according to their sources in order to understand and characterize the materials and physical conditions of their mechanisms of action during an event: [Costa \(1988\)](#), [Hung \(1995\)](#), [Hung et al. \(2001\)](#), [Iverson and Denlinger \(2001\)](#), [Ornelas \(2017\)](#), [Grau Sacoto \(2017\)](#), [Kurovskaia et al. \(2020\)](#) and [Takahashi \(2019\)](#). The debris flow caused by the collapse of the tailings dam in Mariana-MG, Brazil, was recorded by [Ornelas \(2017\)](#). Mitigation or coexistence techniques or measures are processes to reduce

the existing risk of a condition from a high level to an acceptable condition.

2. Methodology

The research evaluated the geotextile tube barrier in a reduced physical model by carrying out experiments that simulate a discharge and the impact of the fluid on the structure and the effectiveness of absorbing the impact and correlating it with the displacements. The main difference between the current research is the barrier's constituent material, which has already been used very successfully in other functions and is highly feasible to build anywhere. Impact containment determines the effectiveness of the system in mitigating the flow of debris from a tailings dam failure.

The simulation of the debris flow that impacts the geotextile tube was initially carried out with water for normalization and better determination of parameters. It was then carried out using fine material and water in a proportion (mass) of >50% solids, characteristics close to the event that occurred in Bento Rodrigues-MG (Ornelas, 2017). The material is homogenized in a mixer until it forms a slurry, which causes the suspension of particles that with the turbulent flow is capable of carrying blocks of rock. By applying the (Kang & Kim, 2015) model, the height and distance to reach the proportional impact pressure were estimated, so the material is raised to a height of 250 cm to generate potential energy and then released onto a conveyor belt with slope segmentations to reduce the dissipation of kinetic energy in vertical impacts on the channel components and change to horizontal flow (the loss of velocity is considered the relevant product of dissipation) and the flow rate and pressure estimate were measured before impacting the structure.

The experiments were carried out with the woven geotextile tube in the isolated condition and tubes in the 3-2-1 stacking condition, filled and installed in the channel on the smooth surface and with the application of liquid petroleum jelly and PVC film, to reduce friction forces on the bottom and side walls. The aim is to analyze the stability of the structure only with the resistance condition of inertia or the difficulty of displacement due to its own weight, however, the friction of the lubricated contact was ascertained.

2.1. Hydraulic Channel

The experimental program was carried out in a circuit consisting of a hydraulic channel with previously established dimensions for a barrier unit section and its displacement, velocity determination and a segmented ramp to direct the flow from vertical to horizontal. There is also a tower to support the tilting reservoir that mixes solids and water, a rigid steel support designed and built to hold the dynamometers and other components designed to record debris flows and the impact on the structure. **Figure 1** shows the channel with the segmented ramp and the tower with the elevated concrete mixer.

2.2. Geotextile Tube Barriers Filling

The geotextile tube barriers were made in isolated and stacked conditions and were ordered with woven geotextiles suitable for the filtration characteristics of the mining tailings obtained for this research. The geotextile tubes were made with a cross-sectional length greater than that of the hydraulic channel. They were filled with the mining waste manually and their masses were obtained and installed in the channel with the ends conformed to the walls after filling to form the debris flow containment barrier.

The tailings used, which come from gold mining, were characterized and the maximum specific weight of the solid particles was determined using the Rice Test equipment with a result of 2.67 g/cm^3 . **Figure 2** shows the graph of the particle size curve.

The research was delimited with 03 types of barrier called BTG 1, BTG 2 and BTG 3. BTG 1 is a simple barrier made up of just one geotextile tube made up of

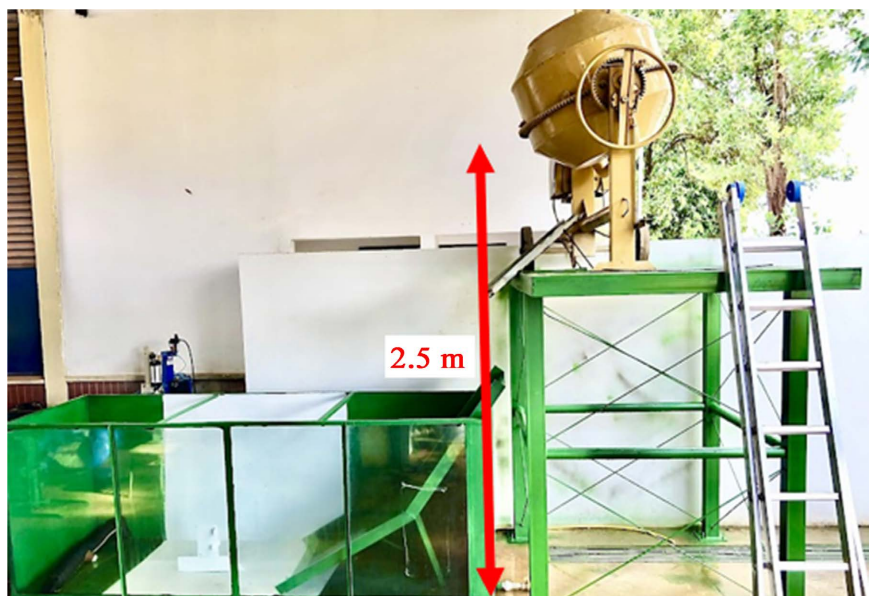


Figure 1. Hydraulic channel, segmented ramp and tower with concrete mixer.

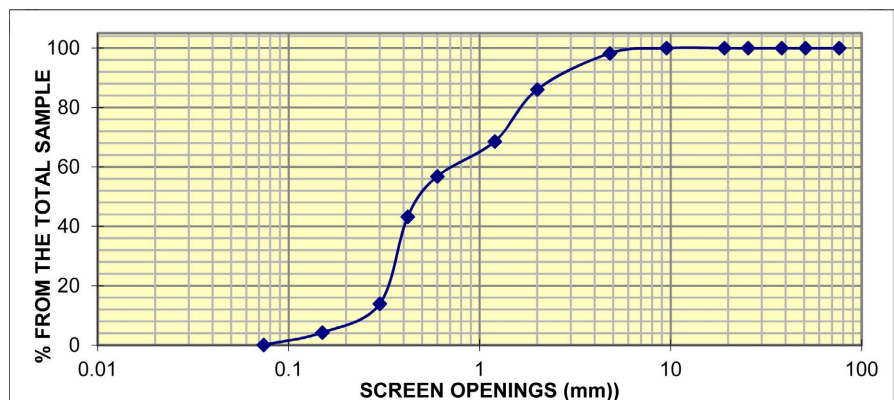


Figure 2. Particle size curve of mining tailings.

the largest tube available, with a diameter of 27.56 cm, as it is the closest to the (Lawson, 2008) ratios, with a shape close to elliptical and the greatest mass. BTG 2 is a barrier made up of a stack of geotextile tubes in a 3:2:1 configuration using 11.46 cm tubes, with 6 segmentations in a pyramidal composition. BTG 3 is also a simple barrier using 17.19 cm tubes, with the purpose of evaluating the variation in the more cylindrical shape and displacements with smaller base area and mass of the barrier.

After filling the tubes, their dimensions were measured and compared with the approximate ratios determined by (Lawson, 2008), as shown in Table 1.

The BTG1 was weighed, obtaining 68.48 kg and moistened where the retention of part of the water used generated an increase in mass resulting in 72.50 kg, which was the value considered in the calculations. It is reiterated that the pieces are free from any fixation and with reduced friction, therefore throughout the test, liquid petroleum jelly was applied to the polished porcelain base and, subsequently, PVC film. Removing and placing the barriers required the use of a crane, as shown in Figure 3, which shows the flow path and equipment, the barrier installed under vaseline with PVC film and the crane.

The maximum static coefficient of friction, μ_e , was determined by the angle at which the geotextile tube left the static state and began to move over a polished porcelain tile like the one installed at the bottom of the hydraulic channel and

Table 1. Comparison of approximate relationships between fundamental and engineering parameters of geotextile tubes according to (Lawson, 2008).

Relations		Geotextile Tube Diameters (cm)					
Engineering Parameter	Theoretical diameter, D_T	11.46		17.19		23.56	
		obtained	reference value	obtained	reference value	obtained	reference value
Maximum filling height, H_T	$H_T \approx 0.55 D_T$	10.50	6.30	15.20	9.45	18.60	12.96
Filled width W_T	$W_T \approx 1.5 D_T$	13.00	17.19	19.80	25.79	28.70	35.34
Base contact width b_T	$b_T \approx D_T$	8.00	11.46	12.00	17.19	18.50	23.56
Cross section areal A_T	$A_T \approx 0.6 D_T^2$	70.00	78.80	150.00	177.30	333.00	333.04



Figure 3. Flow path and equipment, barrier installed under vaseline with PVC film and crane.

also with the application of Vaseline and the same PVC film. The mass of the filled geotextile tube and the contact area of the base were also obtained. The friction value was divided by the applied stress to determine the value of $\mu_e = 0.0003708$, which must be multiplied by the contact area of the base and shoulder in each dam tested.

The reduced physical model, in terms of scale factor, meets the main requirements. The diameter is just one parameter of its dimensions, which interferes with the scale factor in many areas. While the diameter ends up being four times smaller, this engineering parameter being the main dimensional basis, the similarity of the model can be considered analogous to the prototype because the area, length and mass are proportional to the scale. In relation to the tensile strength of the propylene skin fabric, 100 kN/m was used in the two main directions and the highest available today from the same manufacturer is 200 kN/m.

If the skin is more rigid, it can respond more quickly to stresses, but it can be seen that deformations occur to a lesser extent, mainly due to the rigid body movement of the structure (even if flexible) with a high degree of freedom and contact lubrication to reduce friction to values that are not significant enough to generate deformations. The rigidity of the skin is still one of the least influential factors for deformations, as the confined filling material has shear resistance and provides greater rigidity to deformation than the skin. Because there are no restrictions (apart from the reduced static friction at the base), that rigid body movement occurs even in deformable bodies if they do not have any type of restriction (free body movement), where the deformations were limited to the time of application of the impact and therefore not considered.

The necessary and most coherent simplification in this experiment is the direct comparison of the collision, summarized in a peak impact pressure of the debris flow and the reactive or stabilizing forces being the normal force (mass) of the geotextile tube barrier filled with granular material and its inertial response in a free-body condition and the consumption of kinetic energy in internal energy. In this way, a safety factor can be determined. It should be pointed out that due to the combined mass and stiffness of the target (stiffness as a function of pressure application time), in this case the bus, the kinetic energy can be dispersed with little or no deformation, leaving the efforts only for the debris flow, also known in this experiment as the projectile.

2.3. The Safety Factor

The stability of the geotextile tube barrier structure is determined from the factor of safety for the impact pressure so that the barrier absorbs the kinetic energy and accumulates the material from the debris flow. Factor of safety is widely used in geotechnics as an identifier of the level of stability performance when the resisting and destabilizing forces are compared. Authors such as [Marchetti \(2008\)](#), [Das & Sobhan \(2014\)](#), point out that for static retaining structures such as retaining walls and gravity walls, the resistant capacities of the structure are used, obtained by the ratio of the self-weight and friction of the contact with the founda-

tion soil and due to a counter position to the thrusts and tensions generated.

The barrier's safety factor for the stability of the structure was based on what is used in gravity-type containment structures, altering the soil thrust by the estimated impact pressure, and also on the ratio of the sum of resisting forces to the ratio of acting forces. For the resisting forces, the ratio between the self-weight of the dam structure and the geotextile tubes is taken, multiplied by the static friction coefficient corresponding to the contact areas of the barriers (base and shoulders), and for the acting forces, the unit estimate of the normal force of the Impact Pressure generated by the debris flow, multiplied by the area of the barrier wall. Equation (1) presents the numerical relationships and **Figure 4** shows the relationship between the structure's own weight and the impact pressure.

$$FS = \frac{W \times (Ab + Ao) \times \mu_e}{PI \times Ap} \quad (1)$$

where:

FS: Safety Factor

W: Barrier Weight Force

Ab: Base Contact Area

Ao: Shoulder Contact Area

μ_e : Maximum Coefficient of Static Friction

PI: Impact Pressure

Ap: Wall Area

u: Displacement.

The estimated impact pressure was determined using instruments, but can also be obtained using the model established by **Kang & Kim (2015)**. The self-weight of the barrier can be obtained by determining the apparent specific weight of the filling material under confined conditions and by determining the volume of the tubes. The wall is considered to be the surface area to be impacted, perpendicular to the main directions of the estimated impact pressure forces.

The excess displacement (*u*), which indicates the safety factor for the level of failure of the structure, is calculated because the structure is "loose" and has as little friction as possible. In real conditions, even if there is displacement and the barriers are able to accommodate the material coming from the debris flow (progeny/impacting material), they fulfill their function of mitigating the risks

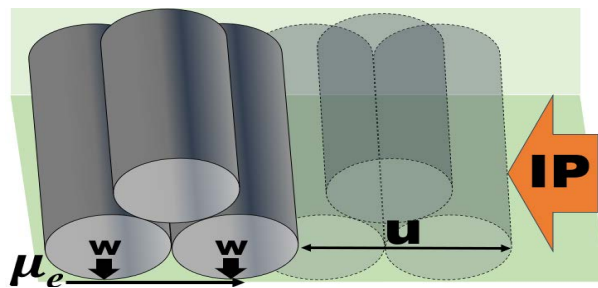


Figure 4. *W* (weight of the barriers), μ_e (coefficient of friction) and *PI* (impact pressure).

so that the relationship between the FS and the displacement indicates the safety limit and determines viability in terms of risk mitigation and the associated potential damage. It is worth noting that the capacity not to be “dragged” by the flow is important if the structure is not to be incorporated into it.

The factor of safety in this experiment does not have conservative relationships, diminishing capacities or extrapolated loads.

The structure may not be stable enough to float, due to the shape of the structure, the flow may impact the base and help the structure to lift and contribute to its potential failure by toppling or sliding, and if the external environment is denser, the barrier could “float”. At equal densities, parts of a segmented barrier can simply be incorporated and continue to “float” with the flow and add to the volume of impacting materials downstream. Other secondary failures analyzed, such as damage to the geotextile and its potential for progressive collapse, did not occur in these experiments.

2.4. Instrumentation and Monitoring

The program of experiments consists of a set of processes to obtain data on the force and tension generated by the impact of the flow, flow velocity and masses of the material constituting the flow and the structure, and the evaluation of the impact on the geotextile tube barriers, failure modes, displacements and deformations. With the dimensional data of the channel, the model of (Kang & Kim, 2015) was applied to predict velocity, flow and pressures and thus organize the instruments to close standards.

Preliminary experiments showed that volume and mass are dependent on velocities > 2 m/s and flow (flow depth $> 40\%$ of height), in order to cause enough impact to cause displacement and rupture of the barrier. Subsequently, increasing the density of the flow and increasing friction were tested.

The velocity was determined by recording the time \times space of 100 cm of the flow, recorded with high-resolution equipment and in slow motion, and for the time, a stopwatch accurate to milliseconds (0.001 s) also recorded in slow motion with the start and end times of the flow. The impact on the structure was also monitored by 02 cameras with a minimum rate of 30 fps (shots per second) and the characteristics and shape of the behavior during the impact were verified.

The mass of a fluid with non-Newtonian behavior in turbulent flow does not follow a pattern; other variations such as flow rate and speed are also variables that influence the impact pressure of the flow. In order to standardize the first experiments and determine the impact pressure patterns versus the deformation of the barriers, it was decided to carry out the experiments only with water and then mix in proportions of clay. **Figure 5** shows three images taken during the water test, the path and turbulent aspect of the impact wave.

The displacements after impact were measured from marks on the channel with a laser tape measure and reading point marks. The rate of displacement is a ratio between the width of the base (L_b) and the distance displaced (D_d) and is measured from reference points in the channel to the front face of the barriers,

obtained by measuring with a laser tape measure.

The pressure generated on the impact face by turbulent flow (of Newtonian fluid or not), has several directions, however, the dynamometer collects a theoretical resultant of the set of forces that impact it for a few seconds, which determines a close estimate of the impact pressure on the structure. The force generated by the flow was collected using two dynamometers with a capacity of 2941.99 N (300 kgf) each, fixed at heights on the rigid steel support and in relation to the bottom of the channel: 1 cm and 5 cm. The sample determination of the possible impact pressure (resulting from the forces) generated by the flow and collected by the dynamometers was carried out at a rate of 40 instantaneous readings per second per dynamometer. Stainless steel shields the size of the cell were made to protect the piezoresistive sensor (strain gage).

The dynamometers are connected to an Arduino® with programming for simultaneous data collection at sufficient intervals and immediate display of load data per cell. The data is transmitted to a laptop via a cable with a USB port where the Parallax software has been programmed to record the load data from cells A and B simultaneously at the same time in a spreadsheet. **Figure 6** shows the process with a dynamometer and an Arduino that collect and transmit data to software on the laptop that records it in a spreadsheet.

The load results were plotted on a loads (cell A and B) \times time graph where it was possible to observe the load variation records with the impact waves, from which the peak load value of the impact waves is taken. This maximum impact pressure load occurs over a maximum period of two seconds and the values can also be compared with velocity, flow and displacements where relevant relationships can be extracted. **Figure 7** shows a graph of an experiment carried out on

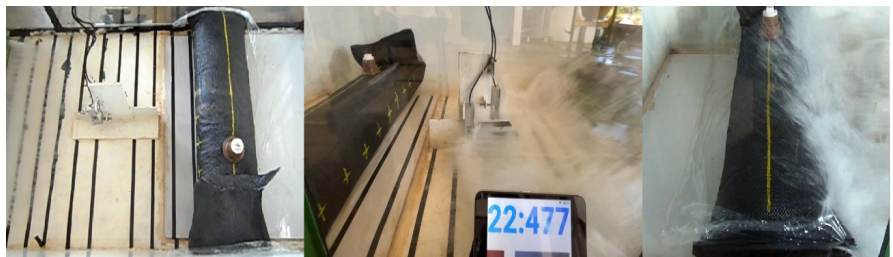


Figure 5. Water test, path and turbulent aspect of the impact wave.

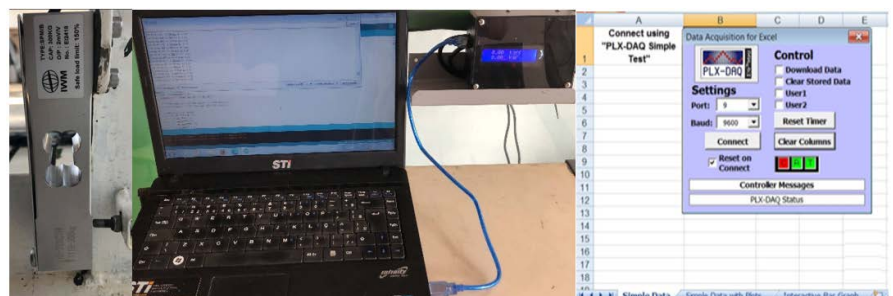


Figure 6. Dynamometer and the Arduino that collects and transmits data to software on the laptop that records it in a spreadsheet.

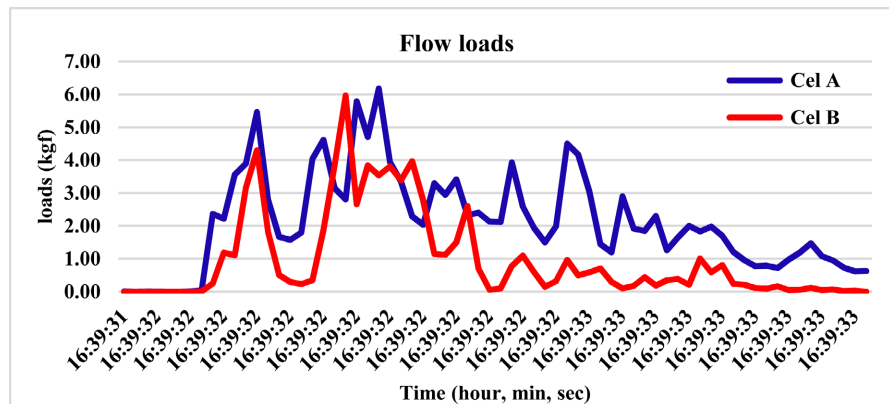


Figure 7. Loads recorded in cells A and B as a function of time.

the loads recorded in cells A and B as a function of time.

The maximum (peak) load is entered into a spreadsheet so that the load can be adjusted by dividing it by the impact area and converting the resultant impact pressure into a unit stress (KPa). The stress multiplied by the impact area can be used to estimate the impact pressure on the structure.

In order to define the single value of the impact pressure, the average of the two samples from the cells fixed at different heights is calculated, and the one placed in the lower position ends up picking up the highest concentrations and peak loads. Only by optimizing the equipment and adjusting the tension calculation (dividing the resulting force by the shield loading area) and checking the flow height in images and landmarks to determine the flow rate, was it possible to arrive at the estimated values.

3. Results and Analysis of Experiments

A structure must meet various criteria such as excessive displacements and deformations, overturning, erosion, overflow, foundation failure, shoulder rupture and overall stability. Several criteria are eliminated in this type of dam because the structure is semi-rigid (or flexible), which guarantees stability even in adverse conditions. In the first experiments, the direct comparison of the normal force generated in the impact of the debris flow and the inertial response of the weight force of the geotextile tube structure, only the extremes were occurring: static stability with inexpressive deformations or the rupture of the structure due to excessive displacement, and therefore this research used the failure mode criterion of excessive displacement. Other failure modes were analyzed, but there were no other failures in the barrier.

3.1. Results of Experiments—BTG 1

BTG 1 is made up of a single 27 cm insulated geotextile tube. In the experiments, it was necessary to promote accommodation to regularize the dimensional differences and maintain a standard, as it ended up with a variation of greater height and smaller width, at one end, otherwise the displacements of the barriers

occurred inclined with higher values on the side with less volume and light and compromised so that where the displacement or rupture inclined the experiments were discarded. This discard condition is validated by the relationship between the contact area and the weight force which generates an increase in the static friction force— μ_e , where even with a smaller base area, a concentration of loads has better efficiency in terms of resistance to inertia, remaining more stable, as the larger base (larger load distribution area) moved more easily.

The data from the experiments and the characteristics of the barriers were entered into a spreadsheet where calculations were made to determine speed and flow. In addition, data was entered on the height of the flow, peak cell pressures and estimated impact pressure and the displacements of the barriers. **Figure 8** shows a graph with the potential trend line (since it is energy), for correlation and the equation corresponding to the control and dependent variables.

It was found that the Safety Factor FS can be a function of the displacement rate. With a quantitative relationship of the admissible displacement up to a limit equilibrium condition can be obtained as a function of the ratio of the mass of the barriers and the estimated impact pressure.

A relationship between the Factor of Safety and the displacement was carried out and from the graph the potential regression showed that between 10% and 15% of the displacement the limit equilibrium occurred and where $FS = 1$. As the FS increases as a function of smaller displacements, the condition of reducing to zero displacement or static stability occurs. **Figure 9** shows the correlation between the FS and the displacement of the BTG1 barriers. It is also possible to see the behavior of the points with a tendency to flow after 10% displacement and the limit range for displacement. It was common in experiments to find the limit of failure as a function of displacement and it was possible to determine that between 10% and 20% displacement of the barrier, with a proportional ratio between the mass of the barrier and the impact pressure applied and regardless of any variation in impact pressure, failure occurred in most cases, suggesting that ruptures or large displacements can occur from these percentages and this ratio, however, excessive displacement may not mean total rupture because, if the bus can dissipate the impact and then the material is retained or minimize any potential damage, the structure will have already fulfilled its purpose.

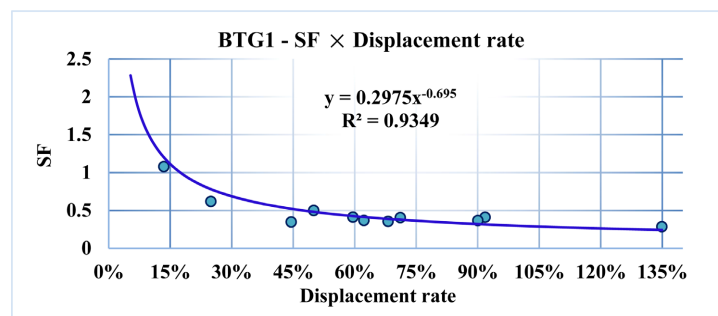


Figure 8. Trend lines of the relationship between weight (W), impact pressure (IP) and Displacement (u).

Sixty-seven experiments were carried out on BTG1, in some of which there were no displacements due to low loading and in most of which the maximum load was sought with the lowest displacement and the limit where the dam broke due to excessive displacement. Only in eight (08) experiments could the data be analyzed after 50% displacement.

For the safety factor, the friction coefficient of the (lubricated) assembly and the contact areas were added, but there was no major change due to the low significance of this parameter and the effectiveness of the reduction. **Figure 9** shows the behavior of the points with a tendency to flow from 10% displacement onwards, based on the displacement and impact pressure relationship.

3.2. Results of Experiments—BTG 2

The BTG 2 is a 3:2:1 pyramidal bus, segmented with six (6) geotextile tubes. The structure is assembled inside the channel for each experiment, after which it is cleaned, the bus is dismantled and the tubes are placed in a vertical position so that the excess water absorbed runs off and can be reused, the cells are dried and the masses are checked after each experiment, and Vaseline and PVC film are applied. **Figure 10** shows the configuration and final shape of the BTG 2 barriers.

Segmentation reduces the mass per geotextile tube and thus improves some transport processes. However, the scale factor means that the tube maintains a shape closer to cylindrical and is therefore more likely not to remain stable in

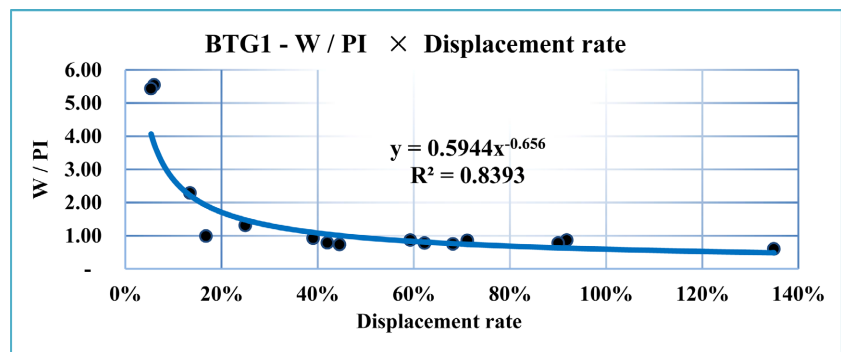


Figure 9. Graph of Safety Factor × BTG1 Displacement.



Figure 10. Configuration and final format of BTG 2.

the free-body condition, especially during impacts. It is possible that pipes in this shape may occur on some construction sites, mainly due to the increased rigidity of the geotextile or the rapid filling process below the water level. The cylindrical shape of the BTG2 geotextile tubes means that there is less contact area between the base and the greater stress and friction coefficient, and the mass of the assembly is greater than BTG1, which results in smaller displacements and greater speed and flow variables.

The data from the experiments and the characteristics of the barriers were entered into a spreadsheet where calculations were made to determine speed and flow. In addition to these, data was entered on the height of the flow, peak pressures of the cells with an estimate of the impact pressure on the dam and the displacements of the dam. **Figure 11** shows a graph with the potential trend line for correlation and the equation corresponding to the control and dependent variables of BTG2.

The correlation of FS with displacement, applying the potential regression of the data, where the limit equilibrium ($FS = 1$) is jeopardized because it occurs with the start of the curve above 10% displacement of the barriers and in many cases after this level of displacement the structure collapses and the risk of the barriers adding more mass transported by the debris flow. **Figure 12** shows the

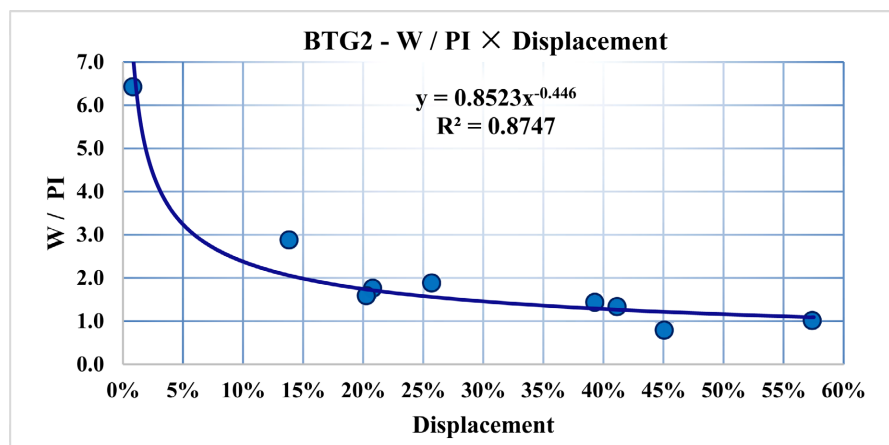


Figure 11. Relationship between Weight (W), Impact Pressure (IP) and Displacement (u).

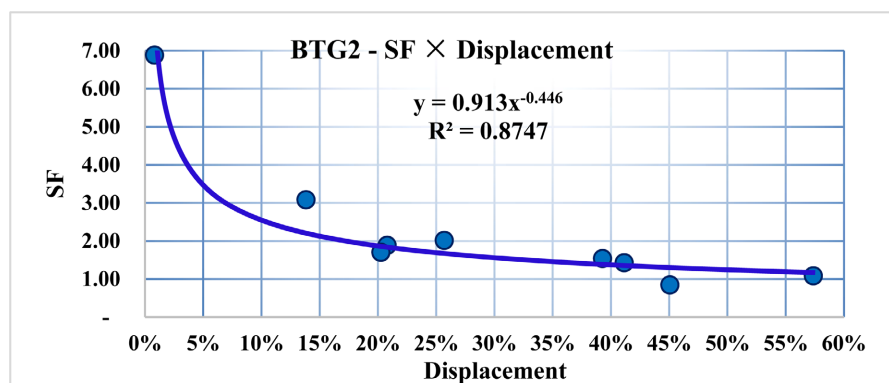


Figure 12. $FS \times$ Displacement rate.

correlation between the FS and the displacement of the BTG2 barriers.

There was not the same possibility of extensive evaluation of W/PI ratios \times displacements as observed in BTG1 from the 50% displacement rate and W/PI = 1, either the dam collapsed at the W/PI ratio < 1 or it moved to the bottom (rupture). Experiments on barriers that collapsed or ruptured and did not provide data amounted to 73.85%. It is suggested that segmented busbars should be tied together so that the parts behave uniformly and avoid collapse.

3.3. Experimental Results—BTG 3

BTG 3 is a simple barrier using a 17.19 cm insulated tube, with the aim of evaluating the variation in form factor and displacements with a lower mass. The structure was assembled inside the channel for each experiment in the same way as BTG1, but with a lower mass and a more cylindrical form factor, it was possible for the structure to collapse even with the use of lower friction by placing Vaseline and PVC film on the polished porcelain tile base. The data from the experiments was entered into a spreadsheet where calculations were made to determine the flow rate and also the peak pressures of the cells were entered to estimate the impact pressure on the dam and its displacements. From this combination of data, it is possible to analyze, process and construct graphs.

Establishing a correlation between the weight of the structure and displacement was difficult and less precise, and after applying potential regression to the data, it was not possible to establish reasonable criteria for limit equilibrium in terms of the relationship between weight, impact and displacement. Even with greater tension in the base due to the form factor (smaller base area), the structure was easy to break due to excessive displacement or the opposite, the absence of displacement, so experiments that do not provide adequate data for formulating failure limits and hypotheses. **Figure 13** shows the correlation between the FS and the displacement of BTG3 and **Figure 14** shows the correlation between the FS and the displacement of BTG3.

With the increase in the static friction coefficient at the base and shoulders of the structure, even with a slight improvement in the correlation of the FS with

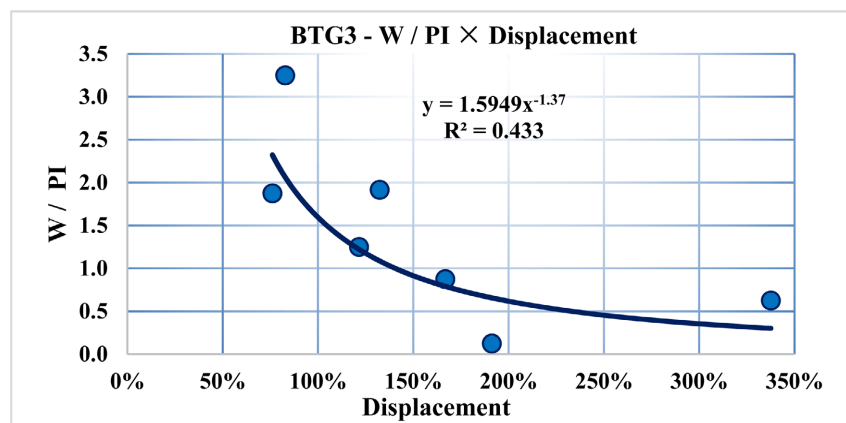


Figure 13. Weight (W), Impact Pressure (IP) and Displacement correlation graph.

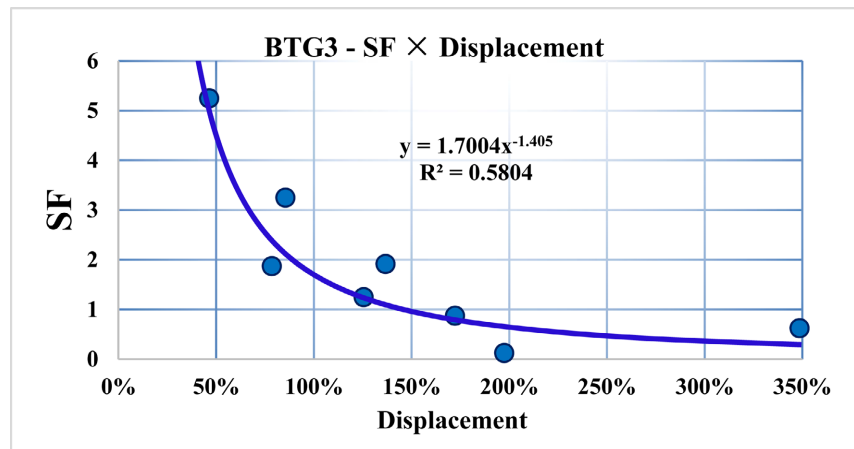


Figure 14. BTG3 FS × Displacement rate.

displacement, the establishment of the FS was seriously impaired where large displacements indicated safety factors above 1.

3.4. Increasing the Coefficient Of Friction and Deformations

The increase in static friction was implemented to check its influence and possible changes in the structure's behavior in relation to this factor. The characteristics of static and kinetic friction are described by Jones & Childers (1993). Friction was increased by attaching a 5 cm wide anti-slip tape, whose measured coefficient is $\mu = 8.26/\text{cm}^2$. Two increments of friction were added, the last with the application of another strip doubling the unit area of static friction. The increase in static friction led to the behavior of the structure in the face of impact pressure where there was either no displacement or rupture at maximum displacement. In this way, the FS is a function of a model in which there can be little or no displacement, only static stability or rupture.

The greater the impact and displacement, the less longitudinal deformation occurred. The maximum deformation in relation to the axis in dry static tests was 20%, while in the experiments the maximum was 3.5%. This demonstrates that mass is the property of a body that specifies how much resistance the body has to changes in its velocity. Experiments show that the greater the mass of a body, the less it accelerates under the action of a given applied force as described by Serway & Jewett (2018). It can also be suggested that maintaining the humidity of the barriers to standardize the mass in the tests can generate suction, which is a resistant increment that increases the rigidity of the barrier to deformations.

3.5. Impact Pressure with Debris Flow

The debris flow was initially predicted to be pulp, mixed in the concrete mixer with a proportion of clay (60%) and water (40%). Until then, it was decided to use only water in experiments to normalize basic and control variables (mainly specific mass of the flow) in tests with busbars in order to provide shorter execution time (preparation, execution, removal and cleaning), avoid damage cells

and mainly the visibility of the flow height and impacted area in the cells to determine the impact pressure estimate.

The flow experiments followed the same processes as the barriers, starting with lower flow rates and lower densities, for experiments with increasing these parameters. The clay and water mixture is mixed in the concrete mixer, which keeps the heavy particles in suspension in a dense pulp similar to mud flows with increasing densities until the addition of crushed stone to form the debris flow. The flow material was recovered and reused in a new experiment with increased flow rate and density. The flow with increasing parameters was possible to establish a manifestation of the water flow with the impact pressure as shown in **Figure 15**, and also a correlation between flow, densities and impact pressure presented in **Figure 16**.

4. Design Criteria for Geotextile Tube Containment Barriers

Design criteria for containment barriers with geotextile tubes vary depending on soil characteristics, site conditions and specific project requirements. However, some common criteria are often considered:

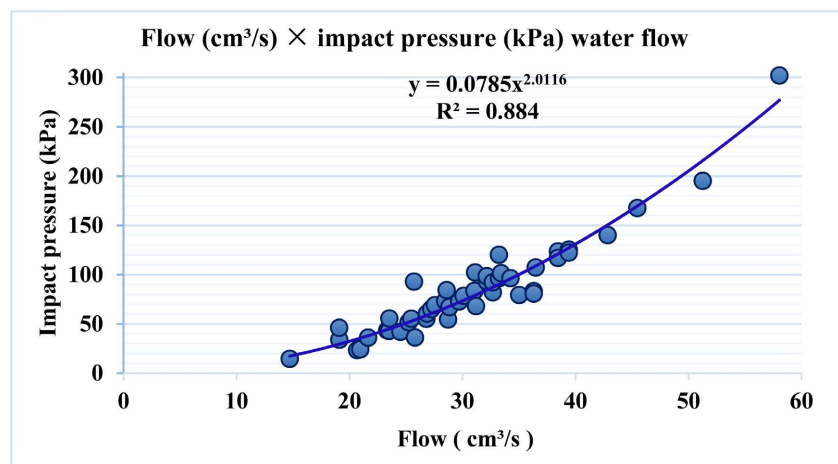


Figure 15. Flow (cm³/s) × Impact Pressure (kPa) for the water flow.

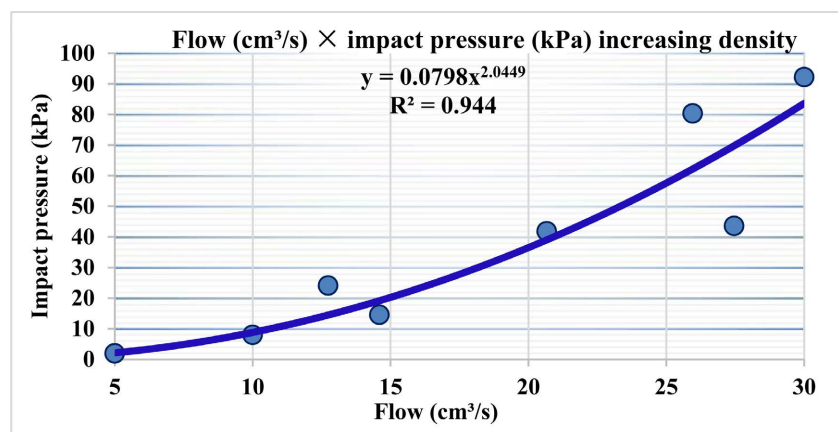


Figure 16. Flow (cm³/s) × Impact Pressure (kPa) and density increase.

Structural stability: Geotextile tubes must be sized to withstand the estimated impact pressure that can be obtained from dambreak information in the case of water dams and from the model established by Kang & Kim (2015) for mining tailings dams. In some cases, after the event, hydrostatic loads and soil pressure are also present, guaranteeing the overall stability of the barrier.

Filtration Capacity: Geotextile tubes must have an adequate filtration capacity to allow water to pass through while retaining the soil particles filling the barriers. This prevents erosion and soil loss through the tube. Also in relation to the laying soil, if the pipe material is too porous in relation to the local soil, it can allow fine particles to pass through, and if the pipe filling material has reduced permeability, it can obstruct the flow of water and impair drainage.

Durability: Geotextile tube materials must be selected to ensure the durability of the structure, resisting chemical, biological and physical degradation over the lifetime of the barrier.

Compatibility with the soil: it is recommended that the geotextile tubes are compatible with the local soil in terms of granulometry, cohesion, angle of internal friction, among other properties. This factor is important because it ensures that the geotextile tubes have an adequate interaction with the surrounding soil, guaranteeing the stability of the containment structure. Compatibility with the soil allows the geotextile tubes to adapt properly to the terrain and loading conditions, ensuring a uniform distribution of stresses and an effective response to variations in the soil over time. If the pipe and soil materials are incompatible, there may be problems with adhesion or load transfer, compromising the stability of the structure.

Flexibility: Geotextile tubes must be flexible enough to adapt to ground irregularities and load variations over time, guaranteeing the stability of the structure. However, for impacts at speeds above 2 meters per second, it has been observed that barriers that were once flexible at the limit of tube deformation enter a transient regime with rigid behavior in the direction of impact.

Ease of Installation: Geotextile tubes should be designed to facilitate installation on site, allowing efficient and safe assembly of the containment structure. Dry filling can be provided for sites where there are difficulties with the water used in hydraulic filling

Compatibility with Reinforcement Elements: When used in conjunction with reinforcement elements such as geogrids or geocells, geotextile tubes must be compatible to ensure effective interaction between the different components of the structure.

Pipe Geotextile: It is recommended to use woven geotextiles where the skin has greater resistance to impacts and perforating or cutting elements in debris flows, which can cause ruptures due to traction, puncturing and abrasion. In general, woven geotextiles tend to be more resistant to these aggressive agents than non-woven geotextiles. This is due to the way the fibers are arranged in each type of material: in woven geotextiles, the fibers are interwoven perpendi-

cularly, creating a more compact and resistant structure than in non-woven geotextiles, where the fibers are arranged randomly and joined by processes such as needling or calendaring.

Feasibility and Use of Large-Scale Barriers

The reduced model was built to test the minimum assumptions for the barrier design principle, starting from a pre-estimated impact pressure and using a correlation for the minimum self-weight of the barrier, reducing friction in contact with the base as much as possible. The feasibility of implementing the barrier implies constructing the safety factor with the real conditions of the barrier installation including friction, contact area and the weight of the barrier. A numerical simulation with this data can adjust and make the structure more precise and safer for use. It is also essential to prescribe the appropriate geosynthetic and filling material.

The feasibility of using the structure can be completed by choosing the best location for installing the barrier, with a competent foundation and fixing options. In the case of protection against failure in a mining tailings dam, it is appropriate to install the barrier after an open valley passage or with a lower slope, to reduce velocity and flow, and with a shorter structure length due to the new narrowing of the channel. The flexibility allows for adaptation even where the foundation is not competent, but analysis must be carried out on overall stability.

The environmental viability is demonstrated by the protection provided in retaining the flow of debris and the mitigation of all the damage that is avoided in addition to the high environmental recovery costs. It is worth noting that geotextile tube barriers can have a cover layer and be integrated into the environmental landscape.

5. Conclusion

Geotextile tubes used as barriers to mitigate risks are feasible, because they can be installed in almost any terrain and filled with the closest materials available, avoiding damage to the environment and integrating into the landscape. This research identified the impact process and the response with the inertial behavior of the structure. The physical models of the barriers were tested extensively until a relationship could be established between different impact values and proportional displacements. In comparison with other barriers, BTG 1 performed best and it is indicated that the elliptical form factor and Lawson's (2008) relationships are the most favorable for designing barriers for this use.

The safety factor was determined only for the stability of a containment barrier in a free body condition and considered the relationship between the self-weight of the barrier structure with geotextile tubes, the coefficient of static friction corresponding to the contact areas of the barriers (base and abutments), and for the acting forces, the unit estimate of the normal Impact Pressure Force generated by the debris flow and multiplied by the projection area (perpendicu-

lar to the flow) of the barrier facing. The data show an excellent correlation between barrier mass and impact pressure and are therefore suitable for first determinations of construction dimensions related to the fundamental parameters of barrier mass and estimation of debris flow impact pressure. The fundamental parameters that influence the impact pressure are the velocity, the flow rate which depends on the depth at the impact site, and the specific weight of the material making up the debris flow, in which case a certain amount of fines is needed to form a slurry with dispersed particles. Only with this condition added to the turbulent flow is it possible to carry blocks of rock at significant speeds that are major impact agents.

The embankment with geotextile tubes showed stability of the structure to overflow, flotation and there was no element that caused damage to the geotextile and its potential for progressive collapse; however, it is possible that this could occur in the event of a continuous flow with cutting elements and for this it can be performed with tubes with the proper geotextile or surface protection.

Acknowledgements

The first author would like to express his gratitude to the University of Brasilia and the Federal Institute of Science and Technology of Tocantins. He would also like to thank Professor Ennio Palmeira for his insight, and the company Huesker for supplying the geotextile tubes for the research and the companies Somatec, King of Steel and Tewel Construction for their support in building the equipment.

Conflicts of Interest

The authors declare no conflicts of interest regarding the publication of this paper.

References

- Costa, J. E. (1988). Rheologic, Geomorphic, and Sedimentologic Differentiation of Water Floods, Hyperconcentrated Flows, and Debris Flows. In V. R. Baker, R. C. Kochel, & P. C. Patton (Eds.), *Flood Geomorphology* (pp. 113-122). John Wiley & Sons.
- Das, B. M., & Sobhan, K. (2014). *Fundamentals of Geotechnical Engineering. Translation of the 8th North American Edition* (562 p.). Cengage Learning.
- Grau Sacoto, C. A. (2017). *Impact Force Analysis of Debris Flows*. Master's Dissertation, UFRJ/COPPE/Civil Engineering Program.
<https://pantheon.ufrj.br/bitstream/11422/9753/1/880617.pdf>
- Hungr, O. (1995). A Model for the Runout Analysis of Rapid Flow Slides, Debris Flows, and Avalanches. *Canadian Geotechnical Journal*, 32, 610-623.
<https://doi.org/10.1139/t95-063>
- Hungr, O., Evans, S. G., Bovis, M. J., & Hutchinson, J. N. (2001). A Review of the Classification of Landslides of the Flow Type. *Environmental & Engineering Geoscience*, 7, 221-238. <https://doi.org/10.2113/gseegeosci.7.3.221>
- Iverson, R. M., & Denlinger, R. P. (2001). Flow of Variably Fluidized Granular Masses across Three-Dimensional Terrain. *Journal of Geophysical Research*, 106, 537-552.

<https://doi.org/10.1029/2000JB900329>

- Jones, E. R., & Childers, R. L. (1993). *Contemporary College Physics*. Addison-Wesley.
- Kang, H., & Kim, Y. (2015). The Physical Vulnerability of Different Types of Building Structure to Debris Flow Events. *Natural Hazards*, *80*, 1475-1493.
<https://doi.org/10.1007/s11069-015-2032-z>
- Kurovskaia, V., Vinogradova, T., & Vasiakina, A. (2020). Comparison of Debris Flow Modeling Results with Empirical Formulas Applied to Russian Mountains Areas. *Open Journal of Geology*, *10*, 92-110. <https://doi.org/10.4236/ojg.2020.101005>
- Lawson, C. R. (2008). Geotextile Containment for Hydraulic and Environmental Engineering. *Geosynthetics International*, *15*, 384-427.
<https://doi.org/10.1680/gein.2008.15.6.384>
- Leshchinsky, D., Leshchinsky, O., Ling, H. I., & Gilbert, P. A. (1996). Geosynthetic Tubes for Confining Pressurized Slurry: Some Design Aspects. *Journal of Geotechnical Engineering*, *122*, 682-690. [https://doi.org/10.1061/\(ASCE\)0733-9410\(1996\)122:8\(682\)](https://doi.org/10.1061/(ASCE)0733-9410(1996)122:8(682))
- Marchetti, O. (2008). *Muros de Arrimo*. Ed Blucher.
- Ornelas, F. S. (2017). *Study of the Physical Vulnerability of Structures Affected by Debris Flows* (148 p.). Master's Dissertation in Geotechnics, Publication G.DM 292/17, Department of Civil and Environmental Engineering, University of Brasilia.
- Pilarczyk, K. W. (2000). Hydraulic and Coastal Structures in International Perspective.
- Serway, R. A., & Jewett Jr., J. W. (2018). *Physics for Scientists and Engineers, V. 1: Mechanics* (Translated by Solange Aparecida Visconte, v. 1. 504 p.). Cengage Learning.
- Takahashi, T. (2019). *Debris Flow: Mechanics, Prediction and Countermeasures* (2nd ed.). Routledge.
- Yee, T. W., Choi, J. C., & Zengerink, E. (2010). Revisiting the Geotextile Tubes at Incheon Bridge Project, Korea. *9th International Conference on Geosynthetics - Geosynthetics: Advanced Solutions for a Challenging World*, 1217-1220.
https://www.researchgate.net/publication/286861159_Revisiting_the_geotextile_tubes_at_Incheon_Bridge_Project_Korea?enrichId=rgreq-9ee6f533b54d796056ea3998f0b511e5-XXX&enrichSource=Y292ZXJQYWdlOzI4Njg2MTE1OTtBUzo0MTQxNTMzODM2NjE1NjhAMTQ3NTc1MzI2OTA4MQ%3D%3D&el=1_x_2